RSC Advances

PAPER

View Article Online
View Journal | View Issue

Cite this: *RSC Adv.*, 2022, **12**, 30480

Upcycling green carbon black as a reinforcing agent for styrene–butadiene rubber materials

So-Hyeon Lee, [a] Jun-Hyun Kim *[b] and Hyun-Ho Park *[a]

Received 24th August 2022
Accepted 18th October 2022

DOI: 10.1039/d2ra05299g

rsc.li/rsc-advances

This study reports the effects of recovered carbon black (produced in a clean and sustainable way) as a reinforcing agent on the physicochemical properties of a styrene–butadiene rubber (SBR) matrix. SBR-based composite materials are prepared with recovered green carbon black (GCB), and these are thoroughly compared to the composite materials containing conventional virgin carbon black (VCB) (produced by the incomplete combustion of petroleum products). The GCB–SBR composite materials generally show detectably inferior properties compared to the VCB–SBR composite under the same preparation conditions due to the limited functionality of the GCB filler. However, the introduction of a small amount of crosslinker, acrylate-functionalized POSS (polyhedral oligomeric silsesquioxane), into the GCB–SBR composite materials effectively enhances the overall physical properties, including the tensile strength, fracture elongation, and thermal stability. The degree of the crosslinking efficiency, thermal stability, and mechanical properties of the composite materials are optimized and thoroughly examined to demonstrate the possibility of replacing typical VCB with GCB, which can allow for upcycling the inexpensive and ecofriendly carbon black materials as effective reinforcing fillers.

Introduction

The conventional fine powder form of carbon black known as virgin carbon black (VCB) is typically produced by the incomplete combustion of petroleum compounds. Given its high surface area and unique physicochemical properties, VCB has been used as an irreplaceable component for various applications, such as in automobiles, plastics, protective coatings, electronics, and the purification industry.[1–4] Recently, much effort has been devoted to find ways to recover carbon black from waste rubber-based products.[5–10] Scrap tires are a serious waste product generated on a global scale. Although these tires have been utilized in various civil engineering applications, including embankments, field drainage, asphalt grip enhancement, and noise reduction in their original state or a crushed form, a large amount of scrap tires (*i.e.*, one quarter of scrap tires) is still being stockpiled or landfilled. An additional recyclable method could be the recovery of carbon black by the pyrolysis of waste tires, which involves a special step where organic matter is heated in either a low-level oxygen atmosphere or a vacuum state.[5,8,11–13] This process readily results in the generation of three main by-products (synthetic gas, liquid fuel, and carbon charcoal). Synthetic gas and liquid fuel are used as fuels, fuel additives, and raw materials for chemical products (*e.g.*, benzene, and limonene). The remaining carbon charcoal can be commercialized as eco-friendly green carbon black (GCB), which is of low value and has shown limited applications. Upon properly refining and/or modifying GCB, it could meet the requirements of technical products in high value applications. In this study, we have developed a strategy to employ GCB as an inexpensive and green filler to reinforce rubber-derived materials whose physical properties can be as good as or better than the composite materials prepared with a conventional VCB filler.

Styrene–butadiene rubber (SBR) is an important synthetic material due to its abrasion resistance and good aging stability.[1,14,15] For diverse applications, SBR-based materials often require fillers to reinforce their original physicochemical properties. Among various reinforcing fillers, carbon black and silica-derived materials have shown positive effects on the overall properties of the resulting SBR-based composite materials.[16–18] This is because simply blending two or more different organic and/or polymeric materials with SBR substances has shown a limited degree of improvement when considering the interactions between the inorganic filler and rubber and/or filler–filler across composite materials.[15,19] The filler–rubber interactions are related to the occlusion degree of the rubber, which is physically combined at fine scales in the filler structure (*e.g.*, carbon black). Such interactions may be observed in a bound rubber that includes aggregates regardless of the elastic part of the matrix.[20,21] However, filler–filler interactions could primarily influence the rigidity of the polymer matrix, where the rigidity could systematically increase as

[a]*Department of Chemistry, Keimyung University, Daegu 42601, South Korea. E-mail: rubchem@kmu.ac.kr*

[b]*Department of Chemistry, Illinois State University, Normal, Illinois 61790-4160, USA. E-mail: jkim5@ilstu.edu*

a function of the filler amount. These overall interactions are determined by new chemical bonds between the filling particle surfaces (filler–filler or filler–rubber matrix), physical attractive forces (*e.g.*, van der Waals forces, hydrogen bonding, *etc.*), the shape of the filler network, and the volume of the fillers.[14,22–24] Even after the introduction of carbon black fillers into SBR materials, the utilization of additional crosslinking agents could further enhance the chemical and physical interactions across the composite materials. Polyhedral oligomeric silsesquioxanes (POSS) are an important class of nanostructure materials that have been successfully introduced in the design of polymeric rubber-based complex systems.[25–29] POSS typically have a 3-D cubic cage structure composed of a Si–O backbone with surface functional groups that can be easily modified with organic moieties to become compatible with a polymer matrix.[30] Upon the incorporation of POSS into polymeric networks, the physical and mechanical properties have shown great improvements in the resulting composite materials due to the reinforcement at the molecular level.[31–33] In addition, surface-modified POSS with unsaturated double bonds (*e.g.*, vinyl and acryl groups) could create new chemical bonds with the rubber matrix and fillers *via* free radical reactions. As such, the effective integration of POSS could potentially improve the performance of rubber-derived composite materials without sacrificing the mechanical properties. It was reported that the use of POSS molecules significantly improves various properties of polymeric materials, including the decomposition temperature, surface hardening, flammability, hydrophobicity, and viscosity reduction.[26,27,34] As such, a fundamental understanding of the nature of interactions between POSS molecules and rubber-based polymer matrices, as well as their impact on thermal, mechanical, and morphological properties, is of great importance.

This study initially involves the characterization of VCB, GCB, and POSS components, as well as their intrinsic roles as reinforcing agents, upon the preparation of SBR-based composite materials. Particularly, the GCB powder used in this experiment was obtained from waste passenger car radial tires that underwent anaerobic digestion and pyrolysis at relatively low temperature, followed by a controlled pulverization process. The proper utilization of recycled carbon black (*i.e.*, GCB) could offer very attractive aspects. For example, GCB as a filler can be economical (*e.g.*, cheaper than VCB), environmentally friendly (*e.g.*, significant reduction of CO_2 during the preparation process), and sustainable supply of carbon materials (*e.g.*, cost is not impacted by the price of crude oil). We also established an effective method to incorporate the reinforcing agents into the SBR. Given the limited surface functionality around GCB, the mechanical properties of GCB-containing SBR were examined to be detectably inferior to VCB-based SBR. After understanding the limited control of physical properties by simply using GCB, properly introducing an additional crosslinker, methacrylate functionalized-POSS, enabled several properties (*i.e.*, crosslinking efficiency, thermal stability, and mechanical properties) of the resulting GCB-containing SBR to be comparable to those of the VCB–SBR composite materials. As such, this study demonstrated the capability of upcycling eco-friendly GCB as an effective filler to reinforce SBR-based materials.

Experimental

Materials and methods

Styrene–butadiene rubber (SBR) as a raw material (SBR1502; 23.5% of styrene content, ML_{1+4} at 100 °C: 52 MU) was acquired from Kumho Petrochemical Co., Ltd (South Korea). The virgin carbon black (VCB)- and green carbon black (GCB)-reinforcing agents used in the experiment were the nonpolluting and high modulus types of semi-reinforcing furnace black, respectively (N774, OCI Co. and 774G-equivalent to VCB, LD Carbon Co., South Korea). Cage-type POSS (MA0735), including eight meta-acrylates in each Si group, was purchased from Hybrid Plastics Co. (USA) and used as received. Additionally, the peroxide-based crosslinking agent, Luperox® F40KEP (1,3-1,4-bis(*tert*-butylperoxyisopropyl) benzene) was purchased from Akema S. A. (France).

Preparation of composite materials

The composite materials were prepared with elements shown in Table 1. To improve the reinforcing effect, cage-type POSS was added to the SBR–GCB mixture (*i.e.*, T-3 and T-4 samples).

A Banbury mixer (Kobe, Japan) was used to thoroughly mix all components prior to the preparation of the composite materials (the detailed mixing process and parameters are shown in Table 2). The initial step involved the addition and mixing of SBR and reinforcing agents in the mixer, after which the resulting mixture was matured at room temperature for 24 h. Finally, the compounds were mixed with a peroxide-based crosslinker and/or POSS in the curing step.

Table 1 Compositions of SBR–carbon black composite materials[a]

Material	T-1 (SBR–VCB)	T-2 (SBR–GCB)	T-3 (SBR–GCB–POSS1)	T-4 (SBR–GCB–POSS2)
SBR raw material	100	100	100	100
GCB	—	40	40	40
VCB	40	—	—	—
POSS	—	—	1	2
Crosslinker (F40KEP)	4	4	4	4

[a] Unit: phr – part per hundred rubber (*e.g.*, 100 g SBR, 40 g VCB, 4 g F40KEP, and 1 g POSS).

Table 2 Mixing process and parameters to prepare the composite materials

Masterbatch preparation
Banbury operating conditions
Mixing speed: 77 rpm
Ram pressure: 3.0 kgf cm^{-2}
Temperature: 60 °C
Cooling water temperature: 18 °C
Fill factor: 0.7
Mixing procedure
1. Add SBR (0.5 min)
2. Add VCB or GCB reinforcing agents (1.5 min)
3. Add remaining additives (1.5 min)
4. Discharge (3.0 min)
5. Cool the samples overnight after removal from the mill
Curing agent addition on a mill (at 60–70 °C)
1. Set the mill opening at 4 mm and add SBR masterbatches from step A (0.5 min)
2. Add peroxide and POSS curing agents (1.5 min)
3. Set the mill opening at 2 mm (1.5 min) and repeatedly cut the sample (~4 times) on each side
4. Set the mill opening at 5 mm (4.5 min)
5. Cool the samples overnight after removal from the mill

Characterization of physical properties

Crosslinking degree of composite materials. Crosslinking of elastomers generally refers to a bond in which two or more polymer chains are connected to each other, and these crosslinks often form a 2-D or 3-D network structure. To examine the crosslinking degree of composite rubber samples, a moving die rheometer (MDR RLR-3 rotorless rheometer, Toyoseiki, Japan) was used to obtain torque values after operating at 160 °C for 50 min with a vibration condition of ±1°. During the MDR measurements, the rheocurve record of the torque applied to the rotor axis served as the basis for determining the crosslinking time of the rubber samples.[35–37] Using the minimum and maximum torque values (T_{max} and T_{min}), the optimal crosslinking time (T_{c90}) was determined. In this study, the optimal crosslinking time based on the crosslinking rate was calculated using the following formula:

$$(T_{max} - T_{min}) \times \text{crosslinking rate (\%)} + T_{min} = T_{c90}.$$

The optimal crosslinking time was determined when the crosslinking rate reached 90%. The scorch time (t_{s2}) was the moment when the minimal torque (T_{min}) increased to 2 lb-in, indicating that the rubber began to undergo the crosslinking reaction.

Mooney viscosity of composite materials. A Mooney viscometer (Vulchem IND Co., South Korea) was used to measure the torque values of the composite materials after mounting them on a rotating metal disk. This rotational viscometer required the preheating (1 min) of a large circular disk sample (38.1 ± 0.05 mm in diameter with a 5.5 ± 0.05 mm thickness), which was then operated at 2 rpm for 4 min at 121 °C according to the ASTM D1646 standard. The Mooney viscosity and scorch time (initial reaction time) were presented as ML_{1+4} (1 min of preheating and 4 min of rotation) and T_5, respectively.[38–40]

Mechanical properties of composite materials. Compression molding was performed on all composite materials at 160 °C after obtaining the optimal crosslinking time determined by an MDR using a flat-plate constant-temperature hydraulic press. The hardness of crosslinked composite materials was measured using a spring-type durometer (Shore A, CL-150, Asker), and their tensile strength and elongation at break were measured by following the KS M6518 standard test procedure. Dumbbell type 3 tensile test pieces were prepared and tested at 25 °C and 500 mm min^{-1} using a tensile tester (UTM; KSU-05M-C; KSU Co., South Korea). The average of each composite sample was calculated using a minimum of five test pieces excluding the highest and lowest values.

Aging test. A Geer-type aging oven was used to examine the thermal stability of composite materials in air. In the oven, a piece of sample (standard Dumbbell type 3 tensile test shape) was mounted on a plate, which was constantly rotated under heated air (100 °C). The thermally-induced aging was carried out for 70 h for all composite samples, which were subjected to the tensile strength measurements. The degree of mechanical strength changes was then compared for all samples. This characterization was followed by Korean Industrial Standards (KS) for physical testing methods for vulcanized rubber (M 6518).

Analysis of reinforcing agents and composite materials. To prepare IR samples, a small amount of VCB and GCB (~1 mg) was mixed with KBr, which was thoroughly crushed using a mortar and pestle. The mixture was transformed into a thin pellet under a pressure of 10^4 H_2O per m^2, which was subjected to molecular vibration measurement by a Fourier transform infrared spectrometer (FTIR; JASCO FTIR-620, Japan). To observe the surface morphology of VCB and GCB, a field emission scanning electron microscope (FE-SEM; JEOL JSM-630F) was utilized at an acceleration voltage of 15 kV.

To determine the presence of the POSS component in the SBR samples, infrared spectra were measured under attenuated total reflection (ATR) conditions. Additional characterizations of POSS were carried out by powder X-ray diffractometry (PXRD; Rigaku RINT 2000, Japan) and nuclear magnetic resonance spectrometry (^{29}Si-NMR, AVANCE III 500; Bruker). A thermogravimetry analyzer (STA 409; Netzsch, Japan) was used to examine the thermal stability of composite materials as a function of time. The temperature-dependent weight loss patterns were monitored under a heating rate of 10 °C min^{-1} from 25 °C to 600 °C in air.

Results and discussion

Prior to characterizing various SBR-based composite materials, each chemical compound (*e.g.*, VCB, GCB, and POSS) was analyzed. Fig. 1 shows the digital photos and FE-SEM images of

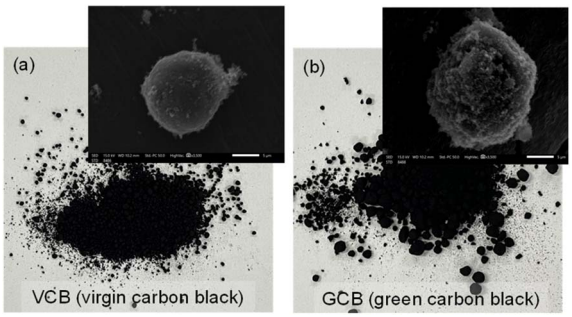

Fig. 1 Digital photos and SEM images of (a) VCB and (b) GCB (scale bar: 5 μm).

the VCB and GCB powder. The VCB sample appeared to be a finer powder as it was produced by the incomplete combustion of petroleum products using a conventional furnace black process. The GCB sample was a slightly coarser and less uniform powder as it was recovered from the waste tires *via* thermal pyrolysis. The SEM images confirmed that the surface of GCB is far rougher and less uniform than that of the VGB sample. The uneven size distribution of carbon black as a filler could cause slightly poorer dispersibility in the polymer matrix to deteriorate the overall mechanical properties. Fig. 2 shows the Fourier transform-infrared spectroscopic (FT-IR) analysis of VCB and GCB as reinforcing agents. The VCB sample shows four distinctive peaks at 3443 cm^{-1} (O–H stretching), 2918/2850 cm^{-1} (CH_2 stretching), 1713 cm^{-1} (C=O stretching), and 1623 cm^{-1} (C=C asymmetrical stretching).[41–43] The reduction of these peak intensities for the GCB sample implies the loss of these functional groups during the recovery process (*e.g.*, reproduced in a clean and sustainable way). We speculated that the lack of these functional groups induced slightly weaker interactions with the SBR matrix where the resulting composite materials exhibited slightly lower mechanical properties than the corresponding composite materials containing VCB. As such, the introduction of an additional crosslinker (*e.g.*, POSS) could enhance the overall physical properties of the composite materials containing GCB (*vide infra*).

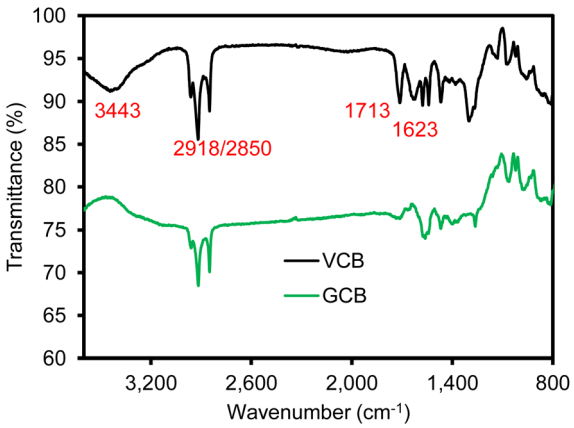

Fig. 2 FT-IR spectra of VCB and GCB.

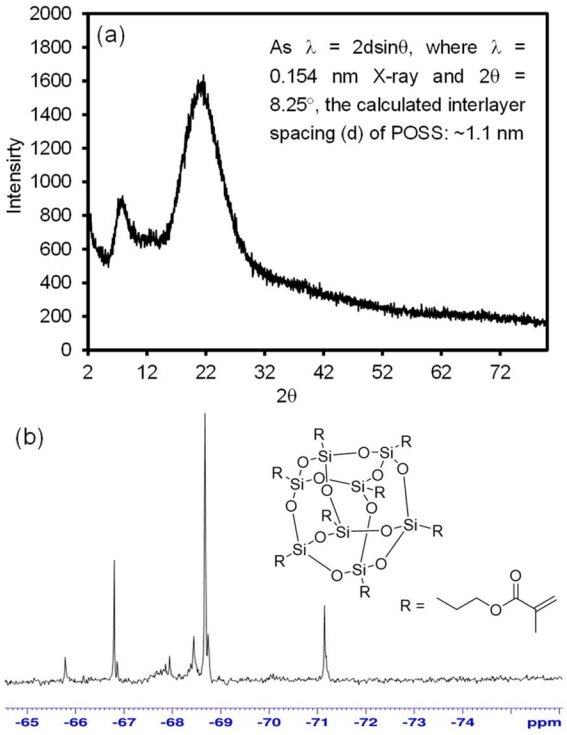

Fig. 3 (a) PXRD pattern and (b) ^{29}Si-NMR of POSS.

The POSS crosslinker was also examined using PXRD and ^{29}Si-NMR prior to preparing SBR–GCB composite materials (Fig. 3). The PXRD of POSS shows two broad 2θ peaks at ~8° and ~22°, which correspond to the cage-like structure and the amorphous siloxane backbone (porous structure), respectively (also explained by previous reports).[29,44–46] Specifically, the calculated *d*-spacing of the first broad peak was around 1.1 nm, which possibly corresponds to the core diameter of POSS molecules. The *d*-spacing for the second broad peak was around 0.40 nm, which could be the distance of the Si–O–Si bond. In addition, the ^{29}Si-NMR spectrum of POSS clearly showed a T^2 peak (partial opening of silicone cage) near −67 ppm and a T^3 peak (silicone cage) near −69 ppm. The presence of these two peaks (T^2 and T^3) from ^{29}Si-NMR is often used to explain the cage-like structure of POSS derivatives.[28,47,48]

The characteristics of SBR composite materials upon the addition of the reinforcing agents (VCB and GCB) and crosslinking agent (POSS) as a function of content are shown in Table 3. The corresponding Mooney viscosity is also shown in Table 4. When the GCB-reinforcing agent was added to SBR, the crosslinking concentration and Mooney viscosity were examined to be higher than when the VCB reinforcing agent was added. With the increasing POSS content from the T-3 to T-4 sample, the crosslinking concentration further increased. When GCB was added, the optimal crosslinking time was extended compared to that of the VCB-reinforcing agent. The increase of the crosslinking degree and viscosity of the GCB-containing SBR composite could be due to a simple physical combination of the SBR matrix and the reinforcing agent caused by the irregular cross-section of GCB. The increase in the

Table 3 Crosslinking characteristics of SBR composites upon the addition of VCB, GCB, and POSS

Mix no.		T-1 (SBR–VCB)	T-2 (SBR–GCB)	T-3 (SBR–GCB–POSS1)	T-4 (SBR–GCB–POSS2)
MDR 160 °C for 50 min	T_{max} (lb-in)	71.0	81.4	79.1	80.0
	T_{min} (lb-in)	17.6	21.4	15.6	13.7
	$T_{max} - T_{min}$	53.4	60.0	63.5	66.3
	T_{c90} (min)	24.43	29.59	32.33	31.53
	t_{s2} (min)	2.04	2.09	2.08	1.54

Table 4 Mooney viscosity of the composite materials[a]

Mix no.		T-1	T-2	T-3	T-4
Mooney viscosity	ML_{1+4} (MU)	45.1	55.8	52.5	50.7
	T_5 (min)	9.25	10.47	10.44	9.27

[a] ML_{1+4}: 1 min of preheating and 4 min of rotation, T_5: initial reaction time.

crosslinking density caused by adding slightly more POSS content improved the crosslinking efficiency across the raw material SBR matrix. In addition, the increase in the POSS content was expected to influence the viscosity (Mooney viscosity; ML_{1+4}) and scorch time (T_5: initial reaction time) of the composite materials. Compared to VCB, the optimal crosslinking time in the presence of GCB was slightly delayed due to the lack of surface functional groups. However, the crosslinking time could be shortened by increasing the amount of the POSS content. It is important to remember that the use of POSS greatly influenced the crosslinking degree and viscosity for GCB-containing composite materials. Further increasing the POSS content (*e.g.*, ≥3 phr) readily resulted in poor miscibility across the SBR matrix when preparing homogeneous composite materials.

After the formation of carbon black containing the SBR composite materials (T-1: VCB–SBR, T-2: GCB–SBR, T-3: GCB–SBR–POSS1, and T-4: GCB–SBR–POSS2), FT-IR spectra were collected (Fig. 4). Although it was somewhat difficult to identify the presence of POSS, the T-3 and T-4 composite materials displayed a slightly stronger peak at 1722 cm^{-1} (C=O stretching) and several peaks at 800–1030 cm^{-1} (Si–O associated stretching and bending). The small shift of the C=O stretching peak could be due to the free-radical polymerization of the acrylate groups in POSS, which is also explained by other group.[33] This observation clearly suggested the crosslinking of POSS across the GCB–SBR samples (*i.e.*, T-3 and T-4).

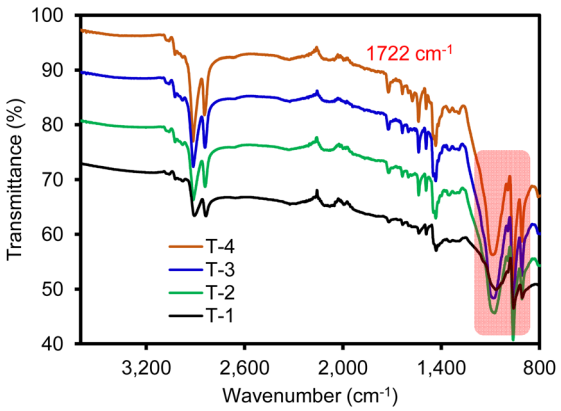

Fig. 4 FT-IR of various composite materials.

Table 5 shows the pyrolysis temperature of the composite materials as a function of weight loss (%), which was examined by a thermogravimetric analyzer. All composite materials exhibited somewhat similar weight loss patterns, but the GCB-containing composites generally slowed down their decomposition rates. Although the presence of POSS did not significantly change the decomposition process of the SBR matrix, increasing the POSS content slightly raised the initial decomposition temperature. This observation indicated that POSS crosslinking could enhance the thermal stability of the SBR matrix. As expected, the composite materials containing GCB had a large amount of residue (*i.e.*, ash) because recovered GCB from waste tires often contains additional impurities (*e.g.*, Al, Cl, Zn, and Si) from the manufacturing process.[43,49–51] The composition of typical VCB is reported by the manufacturers to be more than 95% carbon, with minimal quantities of O, H, N, and S.

The tensile strength and elongation at the break for the composite materials is summarized in Fig. 5. The addition of GCB caused the slight reduction of the tensile strength and elongation of the composite materials. However, these properties gradually increased upon the introduction of POSS, presumably due to the crosslinking effect.[25,52–54] Unlike the use of VCB, the limited surface functionality of GCB could induce weaker attractive interactions across the SBR matrix to unfavourably influence the reinforcing effect. Upon adding POSS, the overall mechanical properties slowly recovered, possibly because the polymerization of POSS could increase the crosslinking density throughout the SBR matrix. The utilization of a small amount of acrylate-functionalized POSS greatly improved the physicochemical properties of rubber-based composite materials containing inexpensive and recovered GCB as a filler that can possibly replace conventional VCB.

The tensile strength of the aged SBR composite containing VCB, GCB, and POSS is summarized in Table 6. After aging at 100 °C for 70 h, the composite materials containing GCB exhibited detectably larger changes of tensile strength. However, the strength changes of these composite materials notably decreased as a function of the POSS content, implying a greatly improved heat resistance. As we mentioned above, the limited functionality around GCB resulted in the less efficient

Table 5 Weight loss (%) of the composite materials as a function of temperature

Composite sample	5 wt% loss temp. (°C)	10 wt% loss temp. (°C)	50 wt% loss temp. (°C)	Residue (%)
T-1	432	439	468	4.5
T-2	439	444	473	5.7
T-3	439	446	476	6.5
T-4	441	445	474	5.9

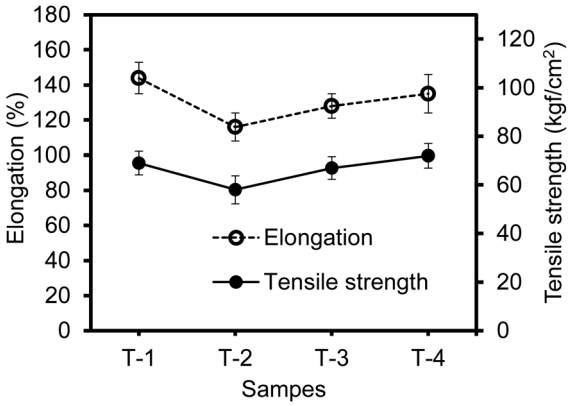

Fig. 5 Mechanical properties of various composite materials.

Table 6 Tensile strength change (%) of the composite materials upon aging at 100 °C for 70 h

Composite sample	T-1	T-2	T-3	T-4
Tensile strength change rate (%)	52 ± 8	60 ± 9	35 ± 5	31 ± 5

physical interactions with the SBR matrix, where the external heat treatment (*i.e.*, aging test) could easily harden the SBR matrix itself to greatly decrease the tensile strength (*i.e.*, larger changes of the tensile strength before and after aging). In contrast, the composite materials containing POSS showed a lower degree of hardness after aging, where the tensile strength fluctuation rate before and after aging was ~30%. As the peroxide-based crosslinker (C–C bond energy between molecules is ~345 kJ mol^{-1}) could play an important role in the preparation of carbon black–SBR composite materials, the use of additional POSS crosslinker possessing Si–O bond (~445 kJ mol^{-1}) across the SBR matrix could result in a slightly higher heat resistance.[55,56] However, the SBR matrix containing POSS still maintained its flexibility, which could be a unique feature for SBR–GCB composite materials (*i.e.*, high flexibility and heat resistance). This observation clearly implied that the use of POSS minimizes the flexibility changes of composite materials, even after 70 h of aging at 100 °C.

Conclusions

SBR-based rubber composite materials were manufactured with VCB and GCB as well as acrylate-functionalized POSS. After examining the characteristics of each filler, thorough analyses were completed to understand the effects of these fillers on the formation and mechanical and thermal properties of the SBR-based composite materials. Unlike conventional VCB, the use of GCB recovered from waste tires exhibiting slightly uneven size distribution and limited surface functionality resulted in somewhat poor interactions across the SBR matrix. Upon the utilization of acrylate-functionalized POSS into GCB-containing SBR composite materials, their overall properties (mechanical properties, thermal stability, and anti-aging property) were detectably improved by increasing the crosslinking density of the entire polymer network. A small amount of POSS plays an important role in positively influencing the degree of cross-linking across the SBR matrix where inexpensive and eco-friendly GCB could serve as a reinforcing filler. As such, GCB could be upcycled as an important filler to replace traditional carbon black materials (*e.g.*, VCB).

Author contributions

Conceptualization: S.-H. Lee, J.-H. Kim and H.-H. Park; methodology: S.-H. Lee and H.-H. Park; investigation and formal analysis: S.-H. Lee and H.-H Park; writing—original draft preparation: S.-H. Lee and J.-H. Kim; writing—review and final editing: J.-H. Kim, and H.-H Park; supervision and project administration: J.-H. Kim, and H.-H. Park; funding acquisition: H.-H. Park.

Conflicts of interest

There are no conflicts to declare.

Acknowledgements

This research was supported by the Bisa Research Grant of Keimyung University in 2021.

Notes and references

1 J. K. Oleiwi, M. S. Hamza and N. A. Nassir, *Eng. & Tech. Journal*, 2011, **29**, 856–870.
2 D. Saini, Gunture, J. Kaushik, R. Aggarwal, K. M. Tripathi and S. K. Sonkar, *ACS Appl. Nano Mater.*, 2021, **4**, 12825–12844.
3 T. Chen, Y. Xie, Z. Wang, J. Lou, D. Liu, R. Xu, Z. Cui, S. Li, M. Panahi-Sarmad and X. Xiao, *ACS Appl. Polym. Mater.*, 2021, **2021**, 5317–5338.

4 M. Roemer, S. T. Keaveney, V. R. Gonçales, J. Lian, J. E. Downes, S. Gautam, J. J. Gooding and B. A. Messerle, *Catal. Sci. Technol.*, 2022, **12**, 226–236.
5 F. Yang, S. Liang, H. Wu, C. Yue, H. Yan, H. Wu, X. Chen, J. Zhang, S. Yan and Y. Duan, *Ind. Eng. Chem. Res.*, 2022, **61**, 6512–6520.
6 L. Yaqoob, T. Noor and N. Iqbal, *ACS Omega*, 2022, **7**, 13403–13435.
7 R. Palos, A. Gutiérrez, F. J. Vela, M. Olazar, J. M. Arandes and J. Bilbao, *Energy Fuels*, 2021, **35**, 3529–3557.
8 N. Nkosi, E. Muzenda, J. Gorimbo and M. Belaid, *RSC Adv.*, 2021, **11**, 11844–11871.
9 L. Chen, L. Wu, L. Song, Z. Xia, Y. Lin, W. Chen and L. Li, *Nanoscale*, 2020, **12**, 24527–24542.
10 E. Burgaz, O. Gencoglu and M. Göksüzoğlu, *Res. Eng. Struct. Mat.*, 2019, **5**, 233–247.
11 J. K. Kim, P. Saha, S. Thomas, J. T. Haponiuk and M. K. Aswathi, *Rubber Recycling: Challenges and Developments*, Royal Society of Chemistry, 1st edn, 2018.
12 P. Toth, T. Vikström, R. Molinder and H. Wiinikka, *Green Chem.*, 2018, **20**, 3981–3992.
13 A. Quek and R. Balasubramanian, *J. Anal. Appl. Pyrolysis*, 2013, **101**, 1–6.
14 G. Akovali and I. Ulkem, *Polymer*, 1999, **40**, 7417–7422.
15 H. Essawy and D. E. El-Nashar, *Polym. Test.*, 2004, **23**, 803–807.
16 F. W. Barlow, *Rubber Compounding: Principles, Materials, and Techniques*, Marcel Dekker Inc., 2nd edn, 1993.
17 A. I. Medalia and G. Kraus, *Science and Technology of Rubber*, Academic Press, 2nd edn, 1994.
18 L. Qu, L. Wang, X. Xie, G. Yu and S. Bu, *RSC Adv.*, 2014, **4**, 64354–64363.
19 R. Faez, W. A. Gazotti and D. Paoli, *Polymer*, 1999, **40**, 5497–5503.
20 S. S. Choi, *J. Anal. Appl. Pyrolysis*, 2000, **55**, 161–170.
21 G. A. Schwartz, S. Cerveny, Á. J. Marzocca, M. Gerspacher and L. Nikiel, *Polymer*, 2003, **44**, 7229–7240.
22 D. J. Kohls and G. Beaucage, *Curr. Opin. Solid State Mater. Sci.*, 2002, **6**, 183–194.
23 J. L. Leblanc, *Prog. Polym. Sci.*, 2002, **27**, 627–687.
24 T. Hüffer, M. Wehrhahn and T. Hofmann, *Environ. Sci.: Processes Impacts*, 2020, **22**, 121–130.
25 J. Zhao, Y. Fu and S. Liu, *Polym. Polym. Compos.*, 2008, **16**, 483–500.
26 T. F. Baumann, T. V. Jones, T. Wilson, A. P. Saab and R. S. Maxwell, *J. Polym. Sci., Part A: Polym. Chem.*, 2003, **47**, 2589–2596.
27 J. P. Lewicki, K. Pielichowski, P. T. De La Croix, B. Janowski, D. Todd and J. J. Liggat, *Polym. Degrad. Stab.*, 2010, **95**, 1099–1105.
28 M. G. Mohamed, M.-Y. Tsai, C.-F. Wang, C.-F. Huang, M. Danko, L. Dai, T. Chen and S.-W. Kuo, *Polymers*, 2021, **13**, 221.
29 E. Omollo, J. Koech, E. Kamalha and V. Adolkar, *Mater. Sci.: Indian J.*, 2017, **16**, 124.
30 G. Pan, J. E. Mark and D. W. Schaefer, *J. Polym. Sci., Part B: Polym. Phys.*, 2003, **41**, 3314–3323.
31 V. Chandrasekhar, R. Boomishankar and S. Nagendran, *Chem. Rev.*, 2004, **104**, 5847–5910.
32 A. Döring, Y. Xiong, Y. Li, J. Schneider, S. A. Cherevkov, E. V. Ushakova and A. L. Rogach, *J. Phys. Chem. C*, 2021, **125**, 15094–15102.
33 H. Zhang, J. Ou, Z. Liu, H. Wang, Y. Wei and H. Zou, *Anal. Chem.*, 2015, **87**, 8789–8797.
34 D. Chen, S. Yi, W. Wu, Y. Zhong, J. Liao, C. Huang and W. Shi, *Polymer*, 2010, **51**, 3867–3878.
35 J. Abraham, H. J. Maria, S. C. George, N. Kalarikkal and S. Thomas, *Phys. Chem. Chem. Phys.*, 2015, **17**, 11217–11228.
36 C. Yin and Q. Zhang, *RSC Adv.*, 2019, **9**, 34330–34341.
37 L. Shao, Z.-Y. Ji, J.-Z. Ma, C.-H. Xue, Z.-L. Ma and J. Zhang, *Sci. Rep.*, 2016, **6**, 36931.
38 V. Krmelová, L. Fusiková and J. Krmela, *Procedia Eng.*, 2016, **136**, 336–340.
39 L. A. Wisojodharmo, R. Fidyaningsih, D. A. Fitriani, D. K. Arti, Indriasari and H. Susanto, *IOP Conf. Ser.: Mater. Sci. Eng.*, 2016, **223**, 012013.
40 A. K. Norizah and S. Azemi, *ASEAN J. Sci. Technol. Dev.*, 2017, **34**, 57–66.
41 N. Hauptman, M. K. Gunde, M. Kunaver and M. Bešter-Rogač, *J. Coat. Technol. Res.*, 2011, **8**, 553–561.
42 C. D. Zappielo, D. M. Nanicuacua, W. N. L. dos Santos, D. L. F. da Silva, L. H. Dall'Antonia, F. M. de Oliveira, D. N. Clausen and C. R. T. Tarley, *J. Braz. Chem. Soc.*, 2016, **27**, 1715–1726.
43 R. I. Sugatri, Y. C. Wirasadewa, K. E. Saputro, E. Y. Muslih, R. Ikono and M. Nasir, *Microsyst. Technol.*, 2018, **24**, 749–755.
44 E. P. Ferreira-Neto, S. Ullah, F. L. S. de Carvalho, A. L. de Souza, M. Oliveira Jr, J. F. Schneider, Y. P. Mascarenhas, A. M. Jorge Jr and U. P. Rodrigues-Filho, *Mater. Chem. Phys.*, 2015, **153**, 410–421.
45 Y.-C. Sheen, C.-H. Lu, C.-F. Huang, S.-W. Kuo and F.-C. Chang, *Polymer*, 2008, **49**, 4017–4024.
46 D. Yaoke, Z. Yuan and J. Wang, *E-Polymers*, 2018, **18**, 237–245.
47 K. Imai and Y. Kaneko, *Inorg. Chem.*, 2017, **56**, 4133–4140.
48 M. Liu, X. Zhang, D. Wang, J. Cheng, X. Pang, W. Qu, C. Li and S. Li, *Polymers*, 2019, **11**, 1953.
49 S. M. R. Costa, D. Fowler, G. A. Carreira, I. Portugal and C. M. Silva, *Materials*, 2022, **15**, 2030.
50 J. Shah, M. R. Jan and F. Mabood, *Energy Convers. Manage.*, 2009, **50**, 991–994.
51 C. G. Robertson and N. J. Hardman, *Polymers*, 2021, **12**, 538.
52 J. Li, H. Wang and S. Li, *High Perform. Polym.*, 2019, **31**, 1217–1225.
53 E. Markovic, S. Clarke, J. Matisons and G. P. Simon, *Macromolecules*, 2008, **41**, 1685–1692.
54 S. Sahoo and A. K. Bhowmick, *Rubber Chem. Technol.*, 2007, **80**, 826–837.
55 Y.-R. Luo, *Comprehensive Handbook of Chemical Bond Energies*, CRC Press, 1st edn, 2007.
56 A. Syakur, H. Berahim, Tumiran and Rochmadi, *TELKOMNIKA (Telecommunication Computing Electronics and Control)*, 2013, **11**, 17–28.